

Structural Impact Mitigation of Bridge Using Tuned Mass

Damper

By

Tu Anh Hoang

A Thesis

Submitted to the Faculty

Of the

WORCESTER POLYTECHNIC INSTITUTE

In partial fulfillment of the requirements for the

Degree of Master of Science

In

Civil Engineering

April 2015

Approved by:

Prof. Yeesock Kim, Thesis Advisor

Prof. Leonard D. Albano, Committee Member

Prof. Pinar Okumus, Committee Member

Dr. Kemal Sarp Arsava, Committee Member

Acknowledgements

I want to thank my advisor, Prof. Yeesock Kim, for his time, guidance and patience with me over the course of my research over the last 3 years. I want to thank Prof. Pinar Okumus for proposing this interesting research topic and for setting up the first steps. Also thank you to Nuoyi Zhu, Jake Hughes and Dr. Kemal Sarp Arsava for giving me valuable feedbacks to complete my thesis.

Abstract

This paper investigates the application of tuned mass damper (TMD) systems to bridge pier systems for structural impact damage mitigation and thus reduce the risk of collapses. A bridge superstructure and substructures are designed in accordance with The American Association of State Highway and Transportation Officials (AASHTO) specifications. A variety of vessel collision forces are obtained from collision testing of a scaled reinforced concrete pier. The optimal parameters of TMD systems are then determined such that the drift and displacement of the bridge superstructure are minimized for various impact scenarios. The structural impact mitigation performance of the pier equipped with the proposed optimal TMD system is compared with five different TMD systems employing the benchmark TMD optimal parameters. The uncontrolled responses are used as a baseline. It was demonstrated from the extensive simulations that the control effectiveness of the proposed TMD system was 25% better than all of the existing TMD models in reducing structure responses.

Table of Contents

1	Introduction	7
1.1	Vibration absorber	7
1.2	Real life application of TMD applications in the civil engineering field	8
2	System modelling	8
2.1	Bridge pier model.....	9
2.2	Bridge Pier equipped with a TMD	12
2.3	Governing equations	13
3	Model Parameters	14
3.1	Setting the scene.....	14
3.1.1	Vessel collision force	15
3.1.2	Bridge design parameters.....	16
3.2	Impact testing	18
4	Optimal design of TMD systems	19
4.1	Parametric study.....	20
4.2	Comparative study and model validation.....	22
5	Hybrid design proposal.....	27
5.1	Design proposal.....	28
5.2	Design coefficients selection and finalization	28
6	Conclusion.....	34
7	References	35

List of Figures

Figure 1: Lumped model of the bridge pier employing a TMD	10
Figure 2: Bridge pier superstructure and substructure	15
Figure 3: Impact testing	18
Figure 4: Sample time history impact force.....	19
Figure 5: Optimal design trends for TMD parameters.....	21
Figure 6: Uncontrolled and controlled deck displacement	22
Figure 7: Uncontrolled and controlled drift	22
Figure 8: Comparison of the proposed TMD and the previous TMDs.....	24
Figure 9: Evaluation criteria as a function of mass ratio	27
Figure 10: Performance criterion J_1 as a function of a coefficient for various mass ratios	29
Figure 11: Performance criterion J_3 as a function of a coefficient for various mass ratios	29
Figure 12: Proposed hybrid design trend	30
Figure 13: Evaluation criteria as a function of mass ratio	30
Figure 14: Time history response of data validation 1	32
Figure 15: Time history response of data validation 2	32
Figure 16: Time history response of data validation 3	33
Figure 17: Time history response of data validation 4	33
Figure 18: Time history response of data validation 5	34

List of Tables

Table 1: Mass of bridge pier substructure and superstructure components	17
Table 2: Stiffness of bridge pier substructure and superstructure components.....	17
Table 3: Damping of bridge pier substructure and superstructure components.....	18
Table 4: Previous optimal designs of TMD	23
Table 5: Uncontrolled Peak Response Quantities of the Structure	24
Table 6: Definition of evaluation criteria.....	25
Table 7: Evaluation Criteria for $\mu=0.03$	26
Table 8: Evaluation Criteria for $\mu=0.05$	26
Table 9: Evaluation Criteria for $\mu=0.1$	26
Table 10: Evaluation Criteria of the Hybrid design for $\mu=0.1$	31

1 Introduction

In the United States, there were 503 bridge failures: 13.73% are directly related to the impact accidents between the bridge and vehicle/barge/ship/tanker, causing multiple deaths (Wardhana and Hadipriono, 2003). Although AASHTO section 3.14 provides guidelines on bridge pier design to protect against vessel collisions, these provisions simply make a stronger pier so that the vessel does not completely take out the pier upon impact. In addition to the AASHTO, different methods are also utilized to protect bridge pier structure against ship collision. Such examples include placing the pier in a safe area that is impossible to be reached by the ship; and installing artificial islands or guide structures (Svensson, 2009). However, all of these methods either are difficult to retrofit the existing structure or do not effectively address all of the potential scenarios of the structure collision events. For example, in an independent research to design protection scheme for a bridge pier, the great water depth prevented protective islands or guide structures. A solution to install floating protection was proposed but then was made impossible by its vulnerability to being pushed underwater by the ships and the corrosion attacked of anchorage devices (Svensson, 2009). There exist other more effective ways to tackle this problem but none has been implemented or even suggested for such purposes: the use of vibration absorber such as tuned mass damper (TMD) is one of the alternative solutions to this problem.

1.1 Vibration absorber

TMD refers to a type of vibration-absorber that consists of a mass that is able to move freely relative to the primary structure. TMDs are used to reduce the amplitude of a structure's vibrations caused by an excessive force. The purpose of this is to prevent damage and complete failure of the structure. The connection between the mass and the structure is usually an elastic spring with a specific stiffness and damping (Sladek and Klingner, 1983). The mass, spring stiffness, and the damping of the TMD are designed in such a way so that when a force is applied, the structure and substructure begin to sway, the TMD will act to mitigate the amplitude of the structural vibrations by the dissipation of energy.

For most cases, TMD systems have been designed for earthquake and wind forces hitting high rise structures such as skyscrapers and telecommunication towers (Sladek and Klingner, 1983). Moreover, they have also been used in automobiles to reduce the vibrations caused when traveling at high speeds and in footbridges to dampen the vibrations caused by excessive walking on the bridge (Dallard et al., 2001). The most notable research work on the design of TMDs with optimum parameters for such applications is from Den Hartog (Hartog, 1956). As the dynamic systems are getting more and more

complex, the formulas have also been updated for different cases (Warburton, 1982; Sadek et al., 1997; Leung and Zhang, 2009).

With a TMD system, the actual bridge vibrations can be mitigated, keeping the primary structural members in its elastic conditions, and thus have a greater chance of preventing a collapse of the bridge as well as reducing downtime for maintenance after any collision (Hoang et al., 2008). In addition to the saving in decreased downtime and maintenance cost, the TMD system could be installed on bridge piers to save the material cost because the newly installed TMD system can provide a better performance without having to design a big strong pier. As a result, it could be used to improve the performance of bridge structure.

1.2 Real life application of TMD applications in the civil engineering field

The actual use of TMD systems is a relatively new concept in civil engineering dating back to just 1976 when a passive TMD system was placed on the CN Tower TV antenna in Toronto, Canada. TMDs have been used in famous buildings such as: the John Hancock Building in Boston, Massachusetts, which was the one of the first building application of a TMD in the United States and in the world, with the two 270000 kg (300t) steel blocks, first installed to reduce discomfort for residence but then found to also reduce wind responses by up to 40% (Sladek and Klingner, 1983; Gutierrez Soto and Adeli, 2013). Probably the most famous bridge employing a TMD is the Millennium Bridge in London, England (Dallard et al., 2001). The largest current TMD in use is in the Taipei 101 building in Taipei, Taiwan which, until 2010, was the world's tallest building (Ctuh.org, 2015). The TMD is placed near the top of the building to reduce vibrations caused by strong winds and earthquakes known to that area.

Despite its wide use in infrastructure systems, there is no research on the application of TMD to bridge piers under vessel collision events. Therefore, this paper is the first to investigate the use of TMD to prevent collapse of bridges due to vessel collisions.

The organization of this paper is as follows: The approach for modeling a bridge structure is presented in Section 2. The optimal design of the bridge equipped with TMD systems is shown in Section 3. The results and the associated analysis are presented in Sections 4 followed by a proposal of a hybrid design with improved performance in Section 5. Finally, Section 6 includes the conclusion remarks.

2 System modelling

In this paper, to demonstrate the effectiveness of the proposed TMD system in mitigating the structural impact responses of bridge structures, a lumped mass bridge pier-deck-TMD model is investigated. The bridge model is first discussed and then the TMD is integrated with the bridge model. Finally, the governing equations of the bridge-TMD model are transformed into state space equations.

2.1 Bridge pier model

A bridge pier model is first derived using the Spring-Mass Model for Barge Flotillas Impacting Bridge Piers proposed by Peng Yuan (Yuan, 2005). In this model, a 2 degree-of-freedom (DOF) reinforced concrete bridge pier is excited by a 15-barge flotilla, which is also simplified as a system of 15 DOF using elastoplastic connections. Several examples and studies were conducted to compare this model with finite element models of different software (LS-DYNA, SAP2000). The results show that despite significantly reduction of computation time (10 minutes by this method and 8 hours by LS-DYNA simulation), the results show similar results of pier displacement in 2 out of 3 examples. In the last example, where the soil, comprising of 5 layers of clayey sands, was also included in the finite element model, the simplified model produced displacement of the pier top 12.7% more than the finite element model (193 m and 171 mm). Due to these reason, it is shown that this model, despite its simplification, provides a good estimation for bridge-pier interaction.

In this paper, the vessel impact forces are replaced by the time-history impact forces measured from the high impact testing facility, and the total number of DOF of the Yuan model is reduced to 2. The reason for this omission of the DOF for vessel/barge in the system is that it significantly increase the system complexity, introducing non-linear behavior of the interaction between the components of the barge. Thus, the computational time for each simulation would be drastically increased – and this approach would not be efficient anymore.

The bridge pier substructure and super structure then are modeled as a 2 DOF model as shown in Figure 1. The 1st DOF includes from the base to the point of impact, and the 2nd DOF is the remaining part of the structure (from the point of the impact to the top of the pier and the deck).

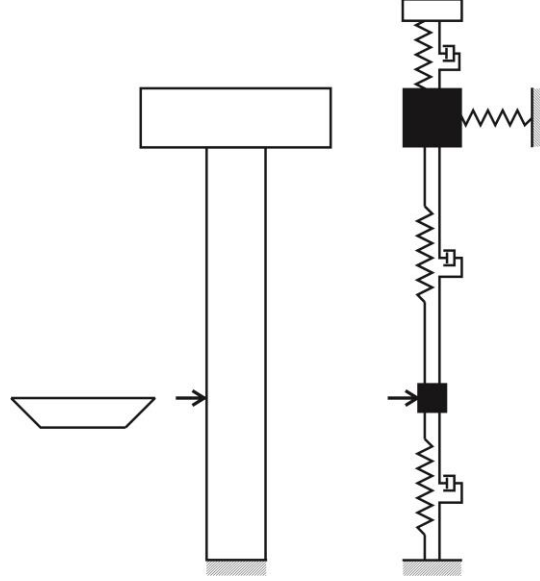


Figure 1: Lumped model of the bridge pier employing a TMD

Initially, each lump mass had 2 DOF: 1 lateral and 1 rotational displacement. Thus, the initial stiffness equation is as follows:

$$EI \begin{bmatrix} \frac{12}{L_1^3} + \frac{12}{L_2^3} & -\frac{12}{L_2^3} & \frac{6}{L_1^2} - \frac{6}{L_2^2} & -\frac{6}{L_2^2} \\ -\frac{12}{L_2^3} & \frac{12}{L_2^3} + \frac{k_x}{EI} & \frac{6}{L_2^2} & \frac{6}{L_2^2} \\ \frac{6}{L_1^2} - \frac{6}{L_2^2} & \frac{6}{L_2^2} & \frac{4}{L_1} + \frac{4}{L_2} & \frac{2}{L_2} \\ -\frac{6}{L_2^2} & \frac{6}{L_2^2} & \frac{2}{L_2} & \frac{4}{L_2} + \frac{k_\theta}{EI} \end{bmatrix} \begin{Bmatrix} x_{M1} \\ x_{M2} \\ \theta_{M1} \\ \theta_{M2} \end{Bmatrix} = \begin{Bmatrix} F(t) \\ 0 \\ 0 \\ 0 \end{Bmatrix}, \quad (1)$$

where E is the Young's modulus of materials, I is the moment of inertia, L_i is height of the i^{th} component of the structure. This model is then converted to a 2 DOF model (1 DOF for each lump mass) by the static condensation (Meirovitch, 1975). The new stiffness matrix K is obtained:

$$K = \frac{3}{L_2^2 \left(3L_1 + 4L_2 + \frac{k_\theta L_2 (L_1 + L_2)}{EI} \right)} \begin{bmatrix} k_{11} & k_{12} \\ k_{21} & k_{22} \end{bmatrix} \quad (2)$$

where

$$k_{11} = \left(1 + \frac{L_2}{L_1}\right)^3 (4EI + (L_1 + L_2)k_\theta) \quad (3)$$

$$k_{22} = 4EI + (L_1 + 4L_2)k_\theta + L_2^2(3L_1 + 4L_2)\frac{k_x}{3} + L_2^3 \frac{(L_1 + L_2)k_x k_\theta}{3EI} \quad (4)$$

$$k_{12} = k_{21} = -2\left(2 + \frac{3L_2}{L_1}\right)EI - \left(1 + \frac{3L_2}{L_1}\right)(L_1 + L_2)k_\theta \quad (5)$$

where k_θ is the rotational stiffness, k_x is the lateral stiffness. The mass matrix is calculated according to the equations:

$$M = \begin{bmatrix} m_1 & 0 \\ 0 & m_2 \end{bmatrix} \quad (6)$$

where

$$m_1 = 0.5(L_1 + L_2) = 0.5L\bar{m} \quad (7)$$

$$m_2 = m_s + 0.5L_2\bar{m} \quad (8)$$

where \bar{m} is the average mass of the pier (mass per length), m_s is the mass of the super structure. Using these parameters to solve for eigenvalues with the assumption that the damping ratio is not so high to affect the natural frequencies, the two natural frequencies are computed as:

$$\omega_{2,1}^2 = R\left(2\lambda^3 + 2\mu\left(1 + 4\kappa + \frac{3\kappa}{\lambda-1}\right)\right) \pm \sqrt{\left(2\lambda^3 - 2\mu\left(1 + 4\kappa + \frac{3\kappa}{\lambda-1}\right)\right)^2 + 4\mu(-3\lambda + 1)^2} \quad (9)$$

where

$$\lambda = \frac{L}{L_1}, \mu = \frac{M_1}{M_2}, \kappa = \frac{L_2^3 k}{12EI}, R = \frac{3EI}{M_1(3L_1 + 4L_2)L_2^2} \quad (10)$$

Finally, damping matrix is defined using Rayleigh's approximation as

$$C = \begin{bmatrix} c_1 + c_2 & -c_2 \\ -c_2 & c_2 \end{bmatrix} \quad (11)$$

where

$$c_i = \alpha_i m_i + \beta_i k_i \quad (12)$$

$$\alpha_i + \beta_i \omega_i = 2\omega_i \xi_i \quad (13)$$

where α and β are the Rayleigh Damping constants.

2.2 Bridge Pier equipped with a TMD

As the pier substructure and superstructure vibrate, the TMDs should be installed in the location that has the most vibration (Hoang et al., 2008). Therefore, the TMD is installed on the 2nd DOF. After the installation of the TMD, the system becomes a 3-DOF system in which the top (or the 3rd) DOF is the TMD. In reality, the TMDs are not necessarily installed on top of the superstructure; it could be installed below the deck for usage convenience. As a result, the new stiffness, mass and damping matrices are defined as:

$$K' = \begin{bmatrix} K_{11} & K_{12} & 0 \\ K_{21} & K_{22} + k_{tmd} & -k_{tmd} \\ 0 & -k_{tmd} & k_{tmd} \end{bmatrix} \quad (14)$$

$$M' = \begin{bmatrix} m_1 & 0 & 0 \\ 0 & m_2 & 0 \\ 0 & 0 & m_{tmd} \end{bmatrix} \quad (15)$$

$$C' = \begin{bmatrix} c_1 + c_2 & -c_2 & 0 \\ -c_2 & c_2 + c_{tmd} & -c_{tmd} \\ 0 & -c_{tmd} & c_{tmd} \end{bmatrix} \quad (16)$$

where K_{ij} is the element of the stiffness matrix in Eq. (2), m_i is the element of the mass matrix in Eq. (6), c_i is the element of the damping matrix in Eq. (11), k_{tmd} is the stiffness of the TMD, c_{tmd} is the damping of the TMD.

2.3 Governing equations

Consider a structure in which the equations of motion are written as

$$M\ddot{u}(t) + C\dot{u}(t) + Ku(t) = F\ddot{u}(t) \quad (17)$$

The second order differential equation of the structure response can be converted into a state space model

$$\dot{u} = Au + BF \quad (18)$$

$$y = Cu + D \quad (19)$$

where

$$A = \begin{bmatrix} 0 & I \\ -M^{-1}K & -M^{-1}C \end{bmatrix} \text{ is the system matrix,} \quad (20)$$

$$B = \begin{bmatrix} 0 \\ -M^{-1}F \end{bmatrix} \text{ is the input matrix,} \quad (21)$$

$$C = \begin{bmatrix} I & 0 \\ 0 & I \end{bmatrix} \text{ is the output matrix,} \quad (22)$$

$$D = \begin{bmatrix} 0 \\ 0 \end{bmatrix} \text{ is the feedforward matrix.} \quad (23)$$

where I is the identity matrix.

3 Model Parameters

With the intention of setting a simulation as realistic as possible in mind, several parameters are derived directly from a bridge design in accordance to the ASSHTO. These parameters are then input into the simulation model for the purpose of designing the TMD. Due to the simplification of modelling and the aim to significantly reduce the computation time, several assumptions were made to define the uncertainties: 1) The point of impact is at 40% from the base of the pier to maximize deflections. This value can vary depending on vessel sizes and water levels 2) All other conditions such as wind load, live load, water wave force, and water damping, are out of the scope of this paper, and thus were neglected.

3.1 Setting the scene

For a realistic investigation the main superstructure and substructure of a 39.624 m (130 ft) long by 11.582 m (38 ft) wide bridge is designed. The bridge has two equal spans of 19.812 m (65 ft) with a pier in the center. The superstructure is composed of a composite rolled steel girders and reinforced concrete slab configuration. There are four W14x370 girders spaced 3.048 m (10 ft) apart with a 1.219 m (4 ft) overhang at each end and the reinforced concrete slab is 20.32 cm (8 in) thick. The following given factors and values are also crucial to the bridge design as well as this TMD investigation: 1) Two CF-PL2 barriers (one running along each of the longitudinal end of the bridge); 2) Weight of the diaphragm beams, shear studs, cross bracing is 437.817 N/m (30 lb/ft) on each interior girder, 291.878 N/m (20 lb/ft) on each exterior girder; 3) Concrete modulus of elasticity = 20.684 GPa (3000 ksi); 4) Steel modulus of elasticity = 200 GPa (29000 ksi). The structure is illustrated in Figure 2.

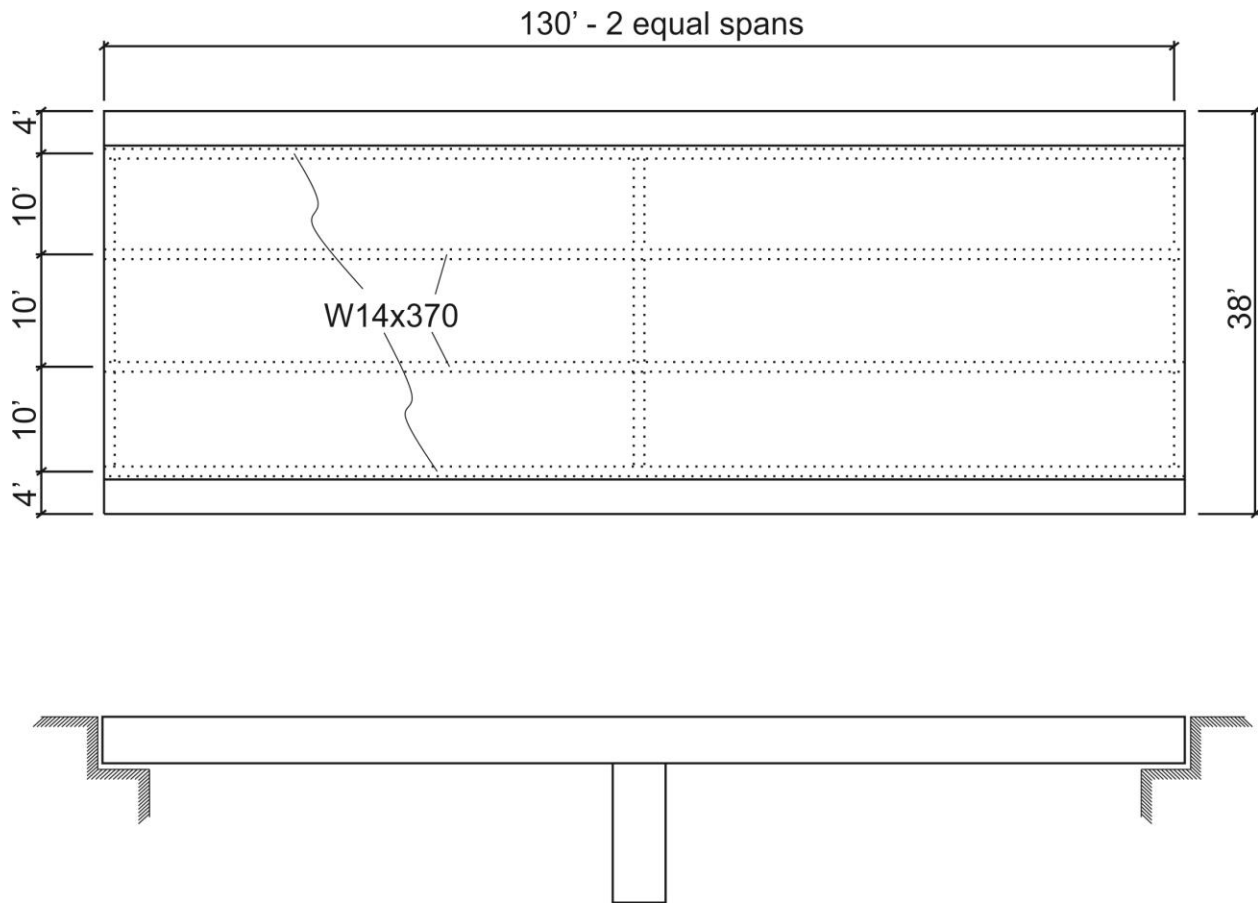


Figure 2: Bridge pier superstructure and substructure

The substructure is a reinforced concrete pier comprised of three 3.394 m (11.135 ft) tall oval columns that are 0.914 m by 1.524 m (3 ft by 5 ft) each having a 0.914 m by 0.65 square meter (3 ft tall by 7 square ft) cross sectional footing with a 1.219 m by 1.067m (4 ft tall by 3.5 ft) wide top slab connecting the 3 piers with the superstructure, the width of the top slab is the width of the bridge (11.582 m or 38 ft). The Mississippi River is one of the most well-known rivers in the United States. Therefore the bridge is fictionally spanning the Mississippi River. It is crucial to choose an actual river for calculating the vessel collision force because average water flow of the river is needed.

3.1.1 Vessel collision force

ASSHTO section 3.14.1 states that a substructure should be designed for a minimum impact force caused by an empty hopper barge that is drifting at a velocity equal to the average yearly current flow at the bridge waterway location (ASSHTO, 2012). The barge is stated to be 10.668 m by 59.436 m (35 ft by

195 ft) that weighs 200 tons empty. The impact force provided in AASHTO section 3.14.8 using the equation 3.14.8-1 is as follows:

$$P_s = 8.15v\sqrt{DWT} \quad (24)$$

where P_s is the impact force in kips, v is the vessel's velocity at impact in feet per seconds, and DWT is the vessel weight in tons. By varying this impact force, different scenarios of vessel size and velocity could be simulated. Following this method, different forces are applied and collected to select the best design for many different collision cases.

As previously stated, the vessel impact velocity is calculated as the average yearly current flow at the bridge waterway location; the vessel impact velocity was taken as the average velocity of the entire river in this paper. This is calculated by dividing the river length by the amount of time it would take to travel the river from start to end. There are competing claims as to the exact length of the Mississippi River which begins at Lake Itasca in Minnesota and ends along the Louisiana shore depositing into the Gulf of Mexico. An average of four lengths from Itasca State Park (4107.05 km or 2,552 miles), the US Geological Survey (3701.49 km or 2,300 miles), the Environmental Protection Agency (EPA) (3733.68 km or 2,320 miles), and the Mississippi National River and Recreation Area (3781.96 km or 2,350 miles) is determined to be 3831.04 km (2,380.5 miles) long. For the average flow rate, it has been shown that it takes roughly 90 days for a raindrop falling into the Lake Itasca to deposit into the Gulf of Mexico (Mississippiriverresource.com, 2015). By dividing the average length by the time to travel the average Mississippi River velocity is determined to be 0.493 m/sec (1.616 ft/sec). This value is verified using information provided by National Park Service, which states that the river velocity is 0.536 m/sec (Nps.gov, 2015). Having all of the needed values, the impact force is calculated as 828.704 kN (186.3 kips).

3.1.2 Bridge design parameters

Once the impact loads are determined, the mass, stiffness and damping parameters should be determined next. Basically, the tributary length for each entity of the bridge deck is the tributary length of the bridge pier (19.812 m or 65 ft) and is applied to the self-weight of each entity. In general, the masses are found by taking the self-weight of each entity of the bridge multiplied by a combination of either the cross-sectional area or the tributary length or both. The calculation results are shown in Table 1.

Table 1: Mass of bridge pier substructure and superstructure components

Component	Mass (kip-sec ² /ft)	Mass (kg)
Concrete Deck Slab Mass	7.948	115992.341
Total Girder Mass	2.988	43606.582
Bracing Mass	2.988	43606.582
Barrier Mass	1.881	27451.132
Total Composite Deck Mass	13.019	190000.000
Pier Mass	6.371	92977.756
Total Mass	19.455	283924.383

Different from the mass, the stiffness is calculated using the model proposed by Yuan: Eq. (2), Eq. (3), Eq. (4), and Eq. (5). The results are shown in Table 2.

Table 2: Stiffness of bridge pier substructure and superstructure components

Component	Stiffness (kips/ft)	Stiffness (N/m)
Bridge pier – lower	1060.900	15482618.721
Bridge pier – upper and composite deck	278.613	4066037.185

Just like the mass, the bridge components are grouped into 2 DOF and their damping are calculated using Rayleigh's damping where α was selected as 0.05, and the associated parameter β was calculated using Eq. (12) and Eq. (13). ξ is the damping ratio which is based on the material type. For steel, the average ξ_S is 0.0004 and for concrete the average ξ_C value is 0.013 (Bachmann, 1995). As these concrete and steel ξ values are different, a value of ξ for each bridge entity was determined by taking a ratio of the masses of steel and concrete in the bridge entity under investigation. ω_i is the natural frequency of the bridge system which can be determined through modal analysis. Table 3 shows the damping values for each entity of the bridge. It is important to note that, similar to the stiffness, the total damping of the composite deck is the damping of the concrete slab and the steel girders. It is assumed that because of the superstructure stiffness, the resisting the impact force is zero, thus, the damping of the superstructure resisting the impact force is also zero.

Table 3: Damping of bridge pier substructure and superstructure components

Component	Damping (kips-sec/ft)	Damping (N-sec/m)
Bridge pier – lower	0.638	9310.878
Bridge pier – upper and composite deck	0.1722	2513.061

3.2 Impact testing

As briefly discussed above, a number of impact tests are conducted to collect the real time impact load data. A single reinforced concrete pier is designed first such that its stiffness is the same with the full scale bridge pier. Then, the impact forces are also scaled down with a scale factor of 1/150. The dimensions of the structural member are 0.25 m x 0.15 m x 0.56 m (9.88 in x 5.93 in x 22.01 in). The 4#3 bars are used as the reinforcing bars. The bridge pier is then loaded underneath a 44482.22 N (10,000 pound) impact tester. One end of the member is clamped in order to act as a fixed end while the other end is left free just like a real bridge pier, as shown in Figure 3. Figure 4 shows a sample data set collected from an impact test.

The similar approach has been done before in the dynamic tests of Meier-Dornberg (Meier-Dornberg, 1983), in which he used a pendulum drop-hammer for the purpose of collecting impact force. There are some pointed out drawbacks, which limit the models from accounting for barge-bridge-soil interaction, important dynamics effect of inertial forces, damping forces and are effects (Cowan, 2007). However, these two setbacks have been solved by the verified lump-mass model by Yuan (2005), allowing the assumption that the model used for simulation in this paper is a linear model.

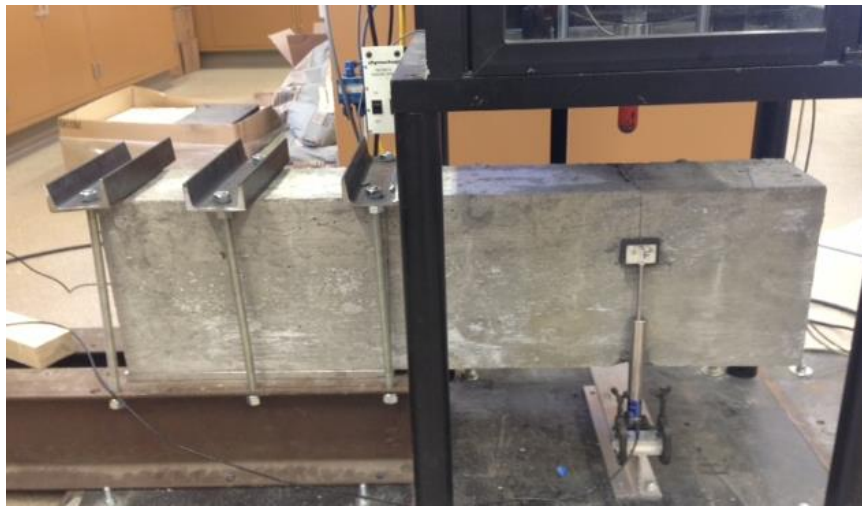


Figure 3: Impact testing

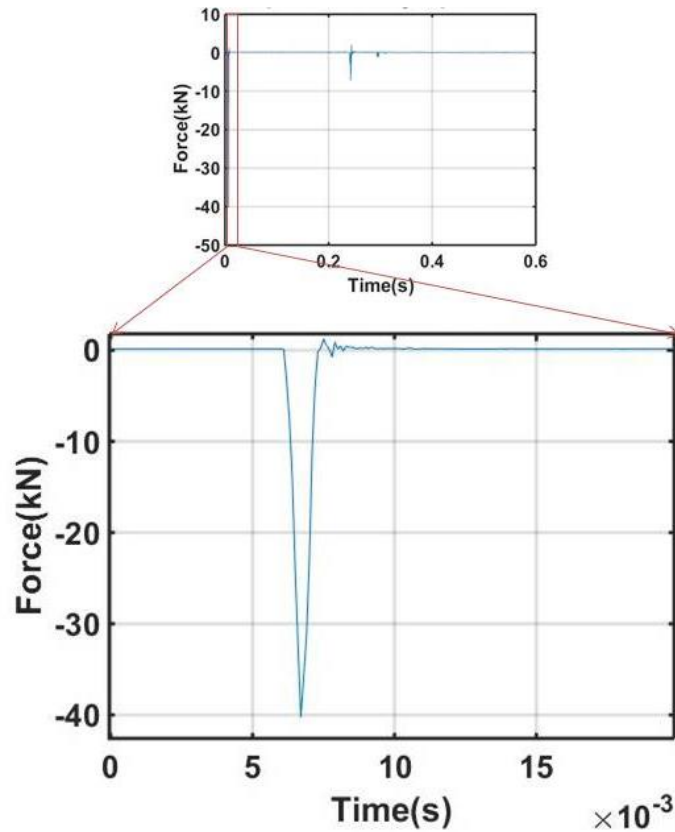


Figure 4: Sample time history impact force

4 Optimal design of TMD systems

A set of impact force signals is used to optimally design the TMD system. Then, the performance of the optimal TMD system is validated using different data sets that are not used for the optimization process. The process of the simulations is summarized as follows:

Step 1: The bridge pier and deck are designed based on AASHTO codes. The full scale model is scaled down and then a laboratory beam model is with same stiffness is used for impact forces data collection by real tests.

Step 2: 145 tests are conducted to collect impact forces.

Step 3: Conduct impact simulations using the scaled down model with different designs of TMDs, with damping ratio and mass ratio ranging from 0 to 20%. Then choose best design cases of the TMD system.

Step 4: The optimized TMD system is validated and updated using evaluation criteria and different impact force data sets that were not used for the training process.

4.1 Parametric study

In this paper, a parameter study-based optimization process is conducted for 140 impact force cases ranging from 8896.443 N to 40033.995 N (2000 lbs to 9000 lbs). For each case of impact forces, 10,000 design case studies of TMDs with varying mass ratios and damping ratios ranging from 0% to 20% are conducted for the performance evaluation. It should be noted that in real scenario, even though the heavier, the more effective TMD is, it is not practical to use a heavy mass that could potentially harm the structure. Hence, the TMD mass is assumed to be between 1% to 10% of the overall structure mass (Farghaly et al, 2012). This value helps engineers focus on designing the damping and spring stiffness. However, the mass ratios from 10% to 20% are still considered in this parametric study to investigate the full potential of the TMD system. The best 0.1% (10 sets of TMD parameters) design that produces the best performance criteria of peak displacement and drift is recorded and selected first to investigate the trend in their parameters of the mass, frequency and damping ratios, as shown in Figure 5. In this figure, the one on the left is the design of optimum TMD frequency as a function of mass ratio, on the right is the design of TMD damping ratio as a function of mass ratio. By taking the median values of all the grey transparent lines (as the results of all the simulations), the solid black line is obtained as the general trends for our design. This trend is then used as our design to investigate its efficiency and performance.

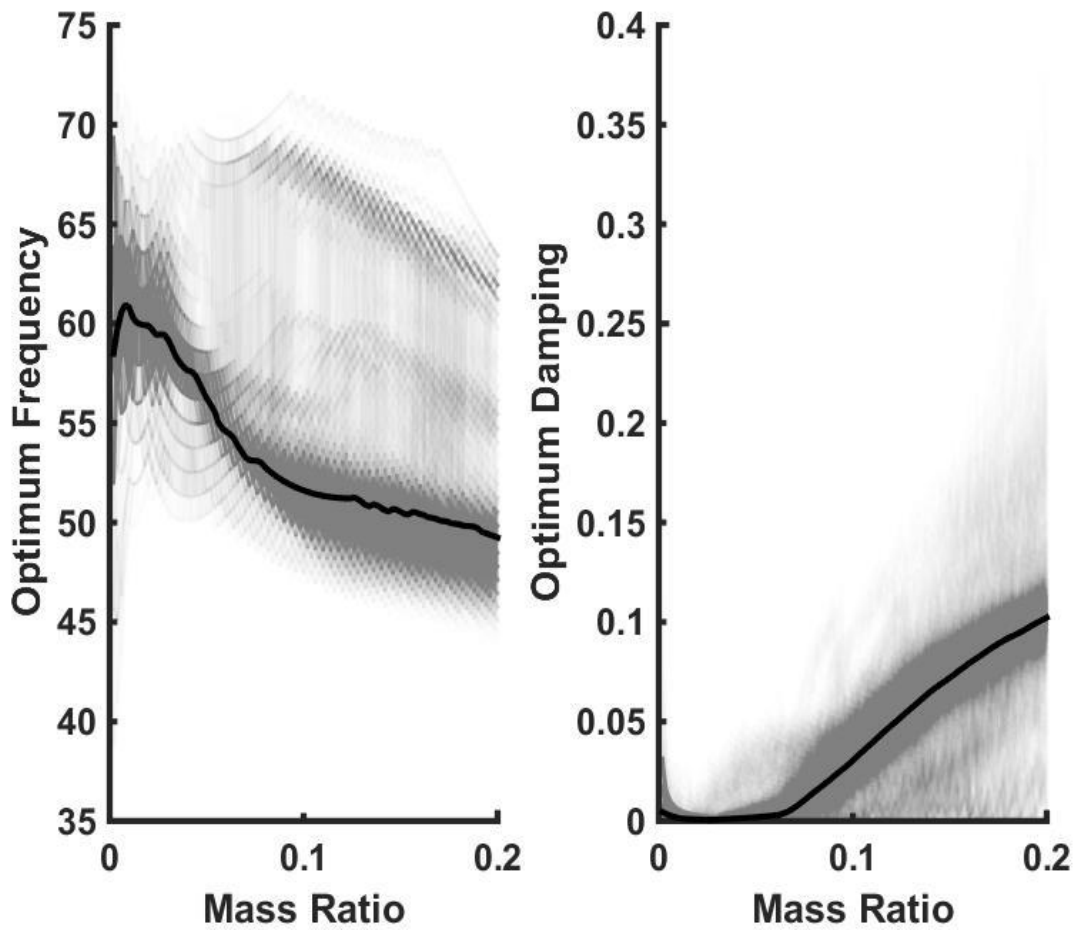


Figure 5: Optimal design trends for TMD parameters

In this paper, the main design criteria include: the minimum deck displacement and the minimum drift between the 1st and 2nd DOF. Figure 6 and Figure 7 show the selected sample control performance of the proposed TMD-pier system under an impact load. Both figures show a good improvement of the structure displacement and drift, especially, the peak response. This performance is then compared against the conventional designs for possible update if necessary.

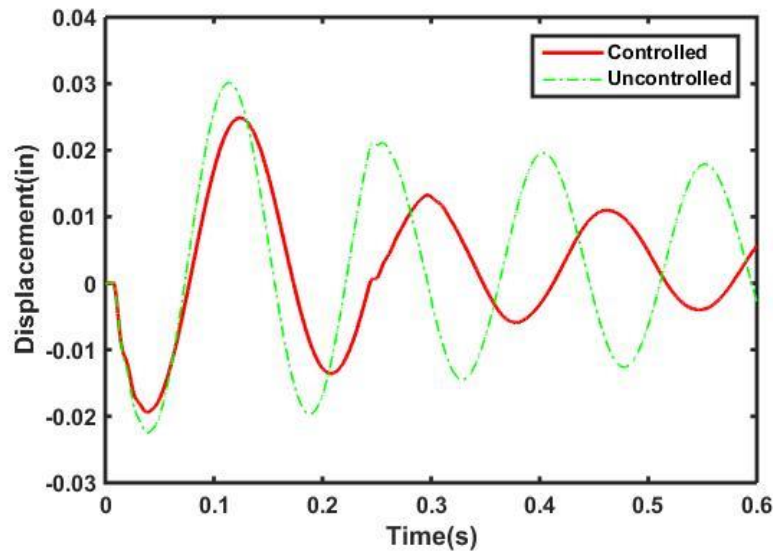


Figure 6: Uncontrolled and controlled deck displacement

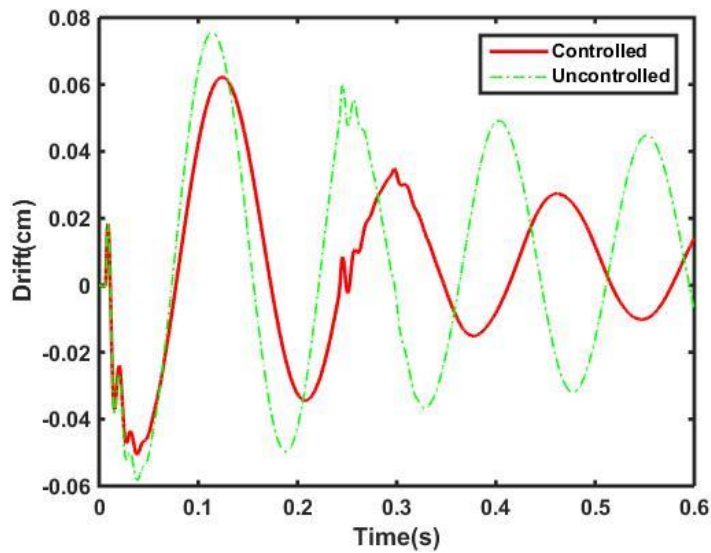


Figure 7: Uncontrolled and controlled drift

4.2 Comparative study and model validation

To further evaluate the performance of the proposed TMD system, the designed TMD system performance is compared with the well-known benchmark models, including Hartog (1956), Warburton (1982), Sadek (1997), and Leung and Zhang (2009), as shown in Table 4. Figure 8 visualizes the parameters of the proposed TMD system with the ones of the benchmark models. It should be noted that

all of these benchmark formulas are derived for either harmonic, earthquake or wind load on a structure. Due to the distinctive initial peak impact force occurring in a much shorter duration than the other types, the objective is to minimize the peak displacement due to this peak force as much as possible. On the other hand, most of the conventional design aims to reduce only the vibration energy of the structure because of the long duration of the earthquake or wind load. Therefore, a distinctive design is expected for this scenario.

Table 4: Previous optimal designs of TMD

Method	$f_{opt} = w_{d,opt} / w_s$		$\xi_{d,opt} = c_{d,opt} / (2m_d w_{d,opt})$	
Hartog, 1956	$\frac{1}{1+\mu}$	(25),	$\sqrt{\frac{3\mu}{8(1+\mu)}}$	(26)
Warburton, 1982	$\frac{\sqrt{1-(\mu/2)}}{1+\mu}$	(27),	$\sqrt{\frac{\mu(1-\mu/4)}{4(1+\mu)(1-\mu/2)}}$	(28)
Sadek et al., 1997	$\frac{1}{1+\mu} \left[1 - \xi \sqrt{\frac{\mu}{1+\mu}} \right]$	(29),	$\frac{\xi}{1+\mu} + \sqrt{\frac{\mu}{1+\mu}}$	(30)
Leung & Zhang, 2009	$\frac{\sqrt{1-(\mu/2)}}{1+\mu} + (-4.9453 + 20.2319\sqrt{\mu} - 39.9419\mu)\sqrt{\mu}\xi + (-4.8287 + 25.0000\sqrt{\mu})\sqrt{\mu}\xi^2$	(31),	$\sqrt{\frac{\mu(1-\mu/4)}{4(1+\mu)(1-\mu/2)}} - 5.3024\xi^2\mu$	(32)

where f_{opt} is the optimum frequency of TMD, $w_{d,opt}$ is the optimum angular damped frequency of TMD, w_s is the natural frequency of the structure, $\xi_{d,opt}$ is the optimum damping ratio of TMD, $c_{d,opt}$ is the optimum damping of TMD, m_d is the mass of TMD, μ is the mass ratio between TMD and structure, and ξ is the damping ratio of structure. Figure 8 compares the optimal parameters of the proposed design with previous studies. As shown in figures, it is observed that the optimal frequency ratio of the proposed impact TMD system is much higher than the previous models while the optimal damping ratio of the collision TMD system is much lower than the benchmark models. This is because the benchmark formulas were derived from the assumption of that the structure is excited by sinusoidal, wind or earthquake loads. It would infer that the parameters of existing TMD systems designed for earthquakes/wind loads should be tuned for structural high impact collision forces.

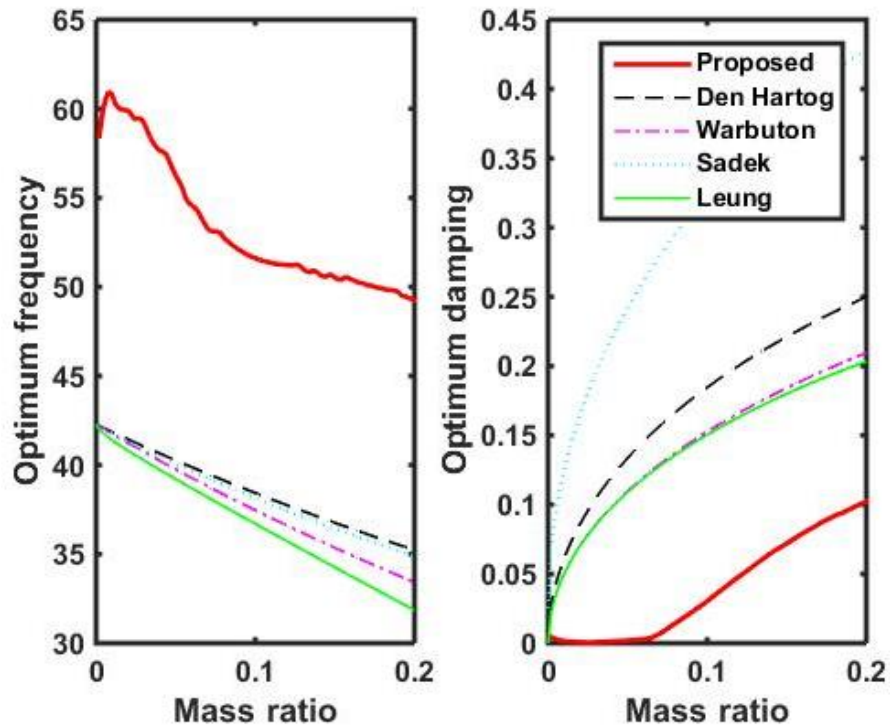


Figure 8: Comparison of the proposed TMD and the previous TMDs

To further evaluate the performance of the proposed system, a design result using the median values of optimum frequency and optimum damping is compared with the design of the four benchmark models in all the 140 impact force cases, using the ASCE structural control benchmark evaluation indices (Spencer et al. 1998). The uncontrolled responses used as baseline for the quantitative analysis results are shown in Table 5.

Table 5: Uncontrolled Peak Response Quantities of the Structure

Criterion	Maximum	Minimum	Mean	Median	Standard deviation
$x_{(cm)}^{\max}$	0.214	0.041	0.135	0.138	0.038
$\dot{x}_{(cm/sec)}^{\max}$	8.038	1.453	4.910	5.088	1.434
\ddot{x}_a^{\max} (cm/sec^2)	2388.563	571.612	1510.195	1567.347	430.882
d_n^{\max} (cm)	0.211	0.041	0.134	0.136	0.038

where $x_{(in)}^{\max}$ is the maximum uncontrolled displacement, $\dot{x}_{(in/sec)}^{\max}$ is the maximum uncontrolled velocity, \ddot{x}_a^{\max} is the maximum uncontrolled acceleration, and d_n^{\max} is the maximum inter-story drift.

The evaluation indices are shown in Table 6.

Table 6: Definition of evaluation criteria

J_1	$\max_{140 \text{ impact force sets}} \left\{ \frac{\max_{t, i \in \eta} x_i(t) }{x^{\max}} \right\}$	for the displacement relative to the ground	(33)
J_2	$\max_{140 \text{ impact force sets}} \left\{ \frac{\max_{t, i \in \eta} d_i(t) }{d_n^{\max}} \right\}$	for the normalized inter-story maximum drift	(34)
J_3	$\max_{140 \text{ impact force sets}} \left\{ \frac{\max_{t, i \in \eta} \ x_i(t)\ }{\ x^{\max}\ } \right\}$	for the normed displacement relative to the ground	(36)
J_4	$\max_{140 \text{ impact force sets}} \left\{ \frac{\max_{t, i \in \eta} \ d_i(t)\ }{\ d_n^{\max}\ } \right\}$	for the normed inter-story drift	(37)

where $\eta = \{1, 2\}$ represents the set of states corresponding to the horizontal displacement.

The results of the evaluation criteria are then computed and shown in Table 7, Table 8 and Table 9 – each represents the result of a different mass ratio μ ($\mu=0.03$, $\mu=0.05$ and $\mu=0.1$, respectively). Figure 9 then sums up the evaluation criteria values for a range of mass ratio from 0 to 20%

Table 7: Evaluation Criteria for $\mu=0.03$

Criterion	Proposed design	Hartog, 1956	Warburton, 1982	Sadek et al., 1997	Leung & Zhang, 2009
J_1	0.9246	0.9495	0.9512	0.9504	0.9492
J_2	0.9254	0.9494	0.9513	0.9503	0.9491
J_3	0.9506	0.7561	0.7467	0.8042	0.7498
J_4	0.9504	0.7556	0.7462	0.8037	0.7493

Table 8: Evaluation Criteria for $\mu=0.05$

Criterion	Proposed design	Hartog, 1956	Warburton, 1982	Sadek et al., 1997	Leung & Zhang, 2009
J_1	0.8803	0.9204	0.9214	0.9242	0.9230
J_2	0.8807	0.9205	0.9213	0.9246	0.9229
J_3	0.9030	0.6971	0.6903	0.7484	0.6949
J_4	0.9028	0.6963	0.6896	0.7478	0.6942

Table 9: Evaluation Criteria for $\mu=0.1$

Criterion	Proposed design	Hartog, 1956	Warburton, 1982	Sadek et al., 1997	Leung and Zhang, 2009
J_1	0.8023	0.8587	0.8626	0.8669	0.8665
J_2	0.7986	0.8590	0.8625	0.8679	0.8663
J_3	0.7830	0.6260	0.6286	0.6691	0.6362
J_4	0.7828	0.6250	0.6276	0.6682	0.6352

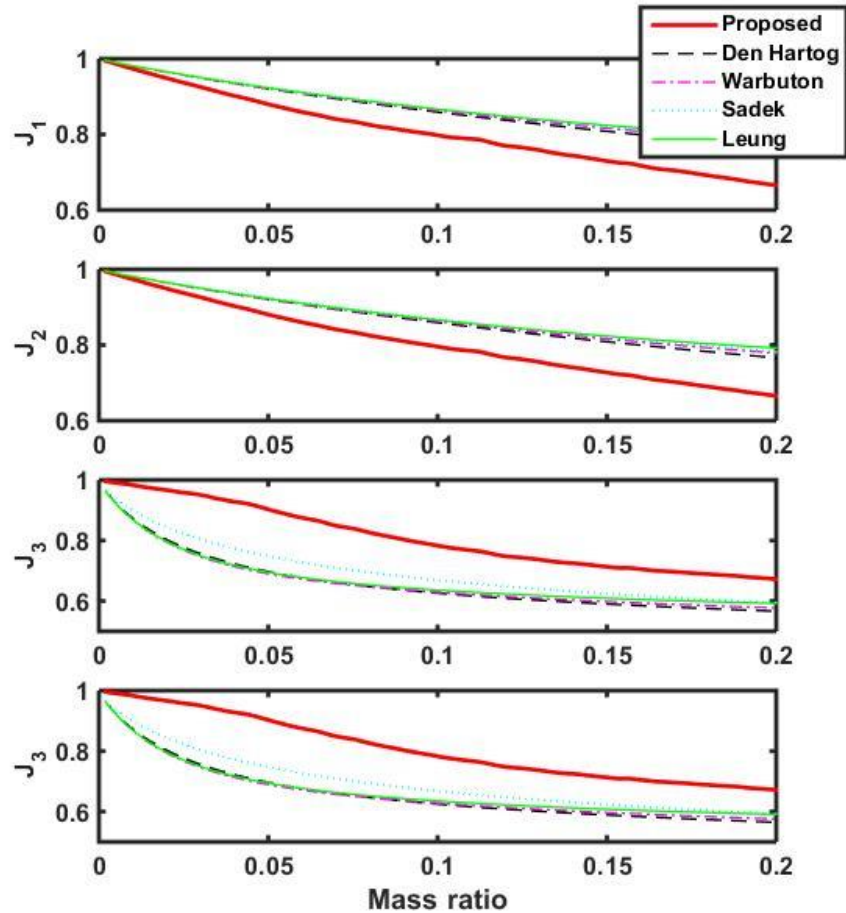


Figure 9: Evaluation criteria as a function of mass ratio

Tables 7, 8 and 9 and figure 9 all show that the main objective of this design has been achieved, which means that the conventional approaches have about the same values of J_1 and J_2 for each mass ratio and all are higher than our approach. However, the disadvantage of using this design is while the peak displacement and drift are significantly reduced, the normed displacement and inter-story drift are worsened, reducing the performance in long term. Therefore, another study to come up with a new design to achieve a better overall performance is necessary.

5 Hybrid design proposal

As observed in figure 9, the proposed design in section 4 is the best in reducing peak displacement and drift of the structure. However, in the criterion of reducing total impact energy over time, it is not. This means as the structure is excited by the impact force, while the member stresses are kept in their elastic region, the whole structure continues vibrating much longer than it should and may fail due to other

reasons. Therefore, it is essential to create another design that satisfies all the criteria, reducing both peak displacement and total energy.

5.1 Design proposal

A second design is then proposed as a hybrid of the 2 designs based on 2 criteria: one is to reduce peak displacement and one is to reduce total impact energy. The design is formulated as follows:

$$\text{Minimize } F = ax_{(in)}^{\max} + b \left\| x_{(in-\sqrt{\text{sec}})}^{\max} \right\| \quad (38)$$

$$\text{Subject to } \begin{aligned} a + b &= 1 \\ a > 0, b > 0 \end{aligned}$$

5.2 Design coefficients selection and finalization

In formula 38, as a and b coefficients change, design of the TMD and performance of the overall objective function change. In addition, as the performance is judged for different mass ratio, the final design and selection of a and b coefficients is totally dependent on the mass ratio of the TMD. In this paper, the mass ratio is assumed to be 10%. Other reference evaluation criteria J_1 and J_3 of 5% and 20% mass ratio are also shown in figure 10 and 11.

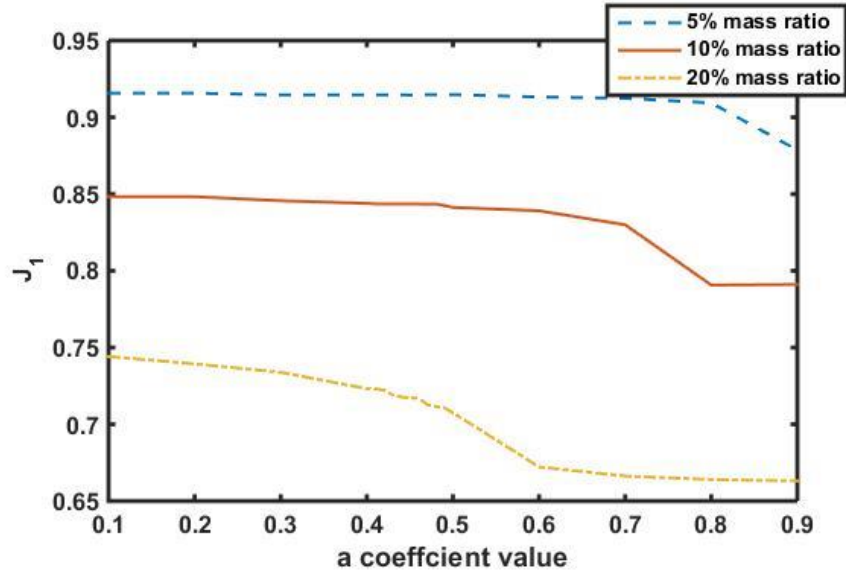


Figure 10: Performance criterion J_1 as a function of a coefficient for various mass ratios

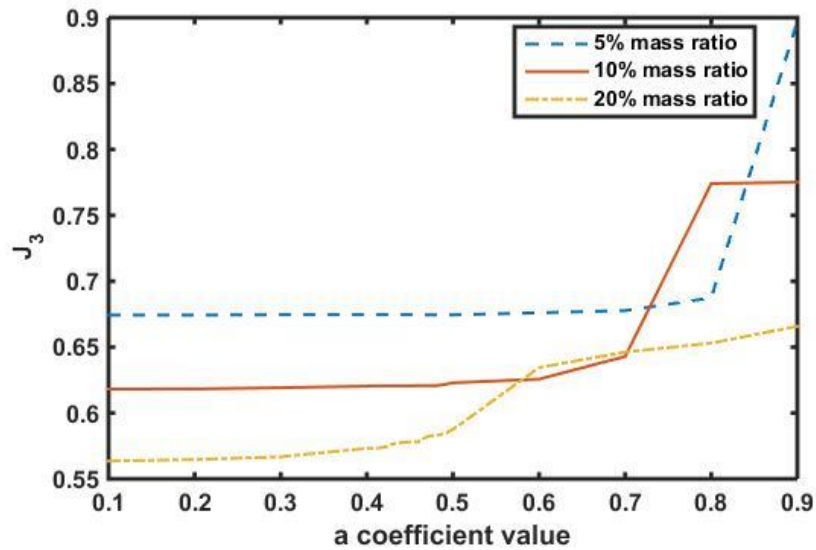


Figure 11: Performance criterion J_3 as a function of a coefficient for various mass ratios

As shown in the two figures 10 and 11, the performance value of J_1 gets closer to the performance of the pure displacement design as a gets closer to 1 (or b gets closer to 0). On the other hand, J_3 gets closer to performance of the pure norm displacement design as a gets closer to 0 (or b gets closer to 1). Another trend to be pointed out is that for mass ratio μ small (5%), the performance doesn't change until a reaches 0.8. This point marking the change for higher mass ratios (10% and 20%) are 0.5 and 0.7, respectively. In this paper, the design is based on 10% mass, thus, the a value is taken as 0.5. The design trends and performance are then shown in figures 12 and 13.

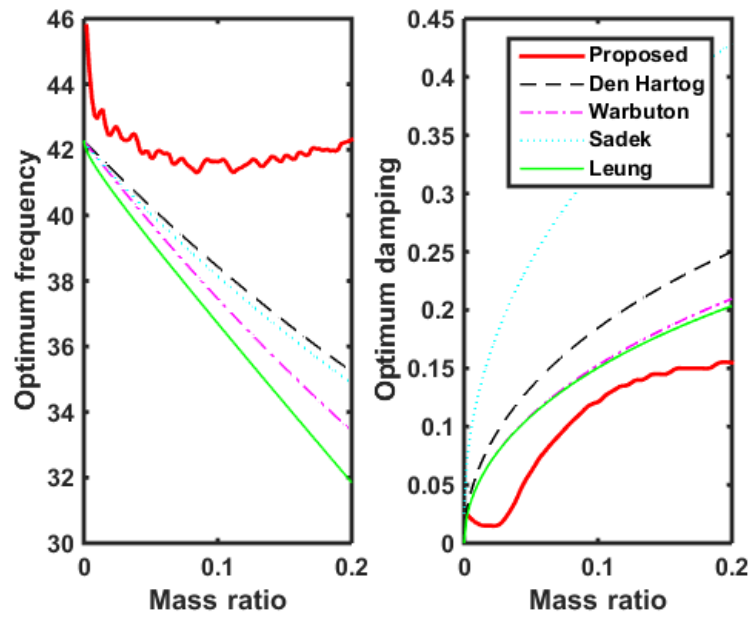


Figure 12: Proposed hybrid design trend

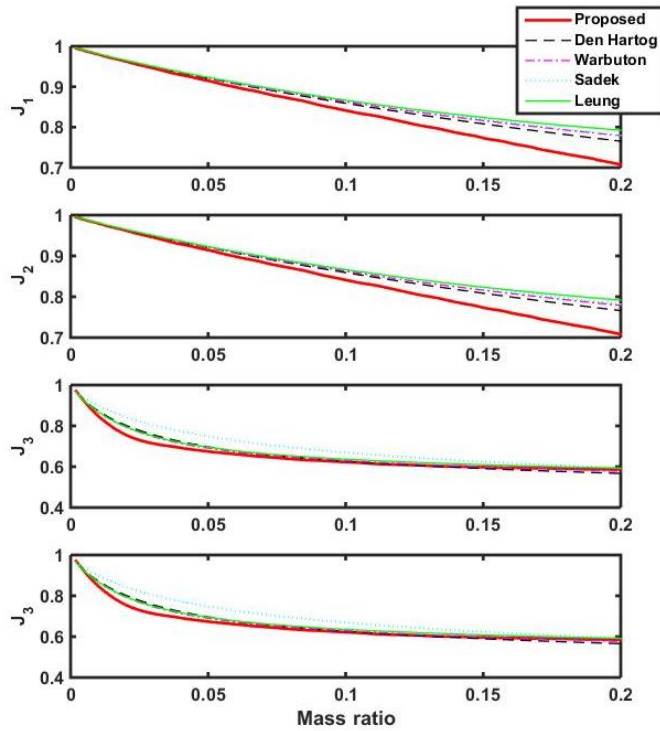


Figure 13: Evaluation criteria as a function of mass ratio

Figure 13 presents evaluation values of J as functions of mass ratios of the new hybrid design. The effectiveness of reducing peak displacement and drift (J_1 and J_2) of the proposed model is proportional to mass ratio. Our proposed TMD system can reduce the peak displacement of the superstructure by maximum of 30% at its full potential (20% mass ratio), while the traditional designs only can reach 22% reduction (25% lower). This difference is critical enough to reduce crack in the concrete and keep the materials from yielding.

One more notable remark in this figure is the superior improvement in the normed value of the displacement and drift. Overall, with this quantitative study, it can be confirmed that our design outperforms all of the conventional designs with significant improvement in peak displacement reduction, which is critical to impact force mitigation. The quantitative study is further investigated and compared against the previous designs is shown in Table 10.

Table 10: Evaluation Criteria of the Hybrid design for $\mu=0.1$

Criterion	Final Hybrid Design	Hartog, 1956	Warburton, 1982	Sadek et al., 1997	Leung and Zhang, 2009
J_1	0.8413	0.8587	0.8626	0.8669	0.8665
J_2	0.8411	0.8590	0.8625	0.8679	0.8663
J_3	0.6229	0.6260	0.6286	0.6691	0.6362
J_4	0.6220	0.6250	0.6276	0.6682	0.6352

Finally, the optimally designed TMD system is tested under 5 different data sets with various peak impact forces for the model validation. These data sets were not used for the TMD optimization process. The testing results of the optimal TMD system with mass ratio of 10% under this data set are shown in Figure 14 to Figure 18. It could be seen that the proposed hybrid TMD is very robust in reducing both peak and normed displacement and drift of newly untrained impact excitation.

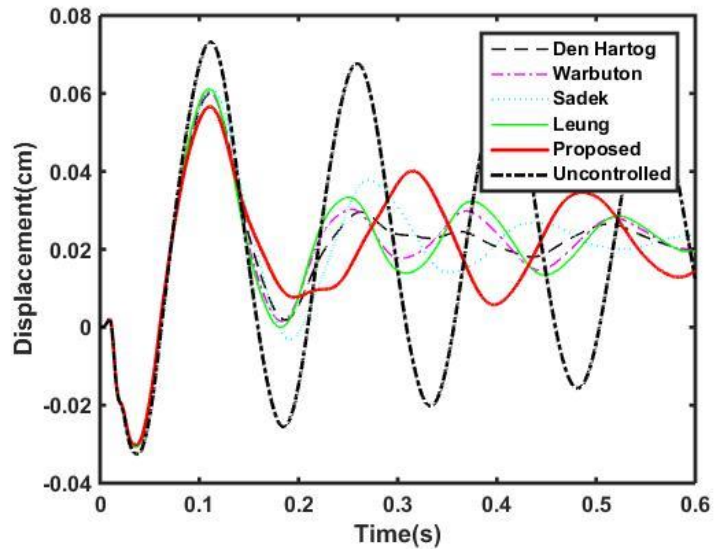


Figure 14: Time history response of data validation 1

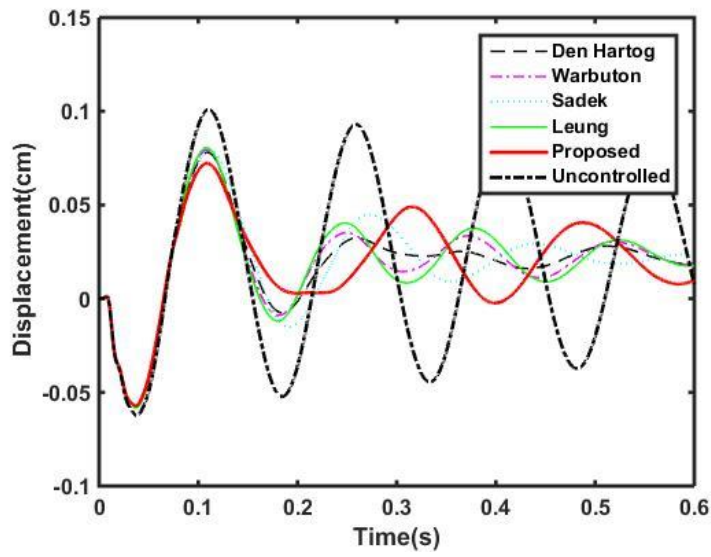


Figure 15: Time history response of data validation 2

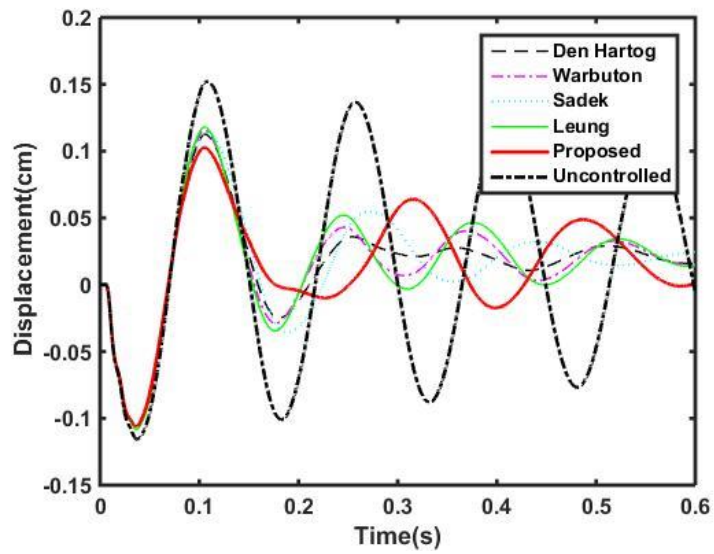


Figure 16: Time history response of data validation 3

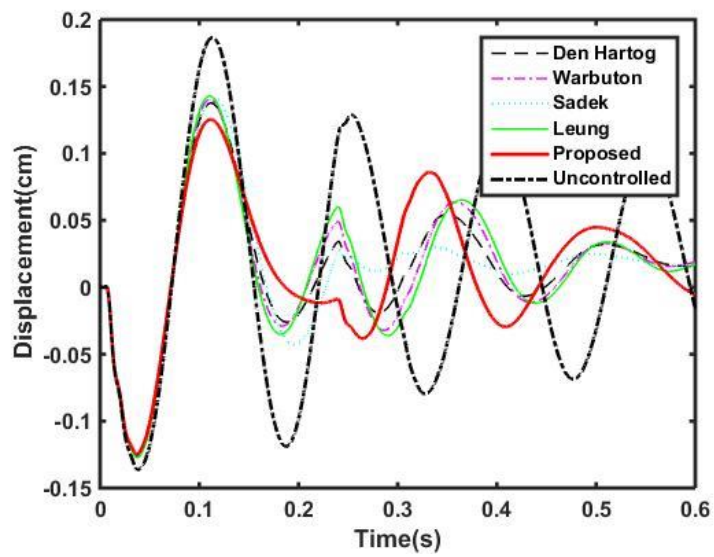


Figure 17: Time history response of data validation 4

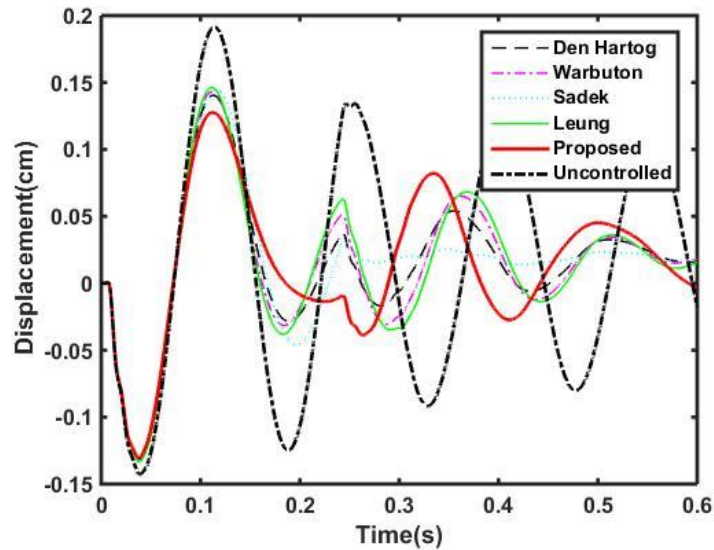


Figure 18: Time history response of data validation 5

6 Conclusion

In this paper, the use of TMD for structural impact hazard mitigation has been proposed. To demonstrate the proposed TMD system, a reinforced concrete bridge pier structure under a variety of impact loads was investigated. Based on the measured impact loads, a TMD parameters were optimally determined such that the peak displacement and drift of the structure are minimized, keeping the structural elements in their elastic conditions while maintaining an acceptable vibration energy reduction. The optimum TMD system was validated using different structural control evaluation criteria and impact loads that were not used in the optimization process. The effectiveness of the proposed optimal TMD system was compared with the ones of four different benchmark TMD models. The uncontrolled bridge pier system was used as a baseline. It is demonstrated from the optimization processing and testing results that the use of TMD is a successful method to mitigate the response of bridges due to vessel collisions and thus reduce the chance of damage and complete collapse. The simulation results also showed that the proposed hybrid optimal TMD system is more effective in mitigating structural impact responses than all the benchmark designs. Using the proposed TMD could improve the performance drastically by about 25%, which in some situation, could prevent the structure from cracking and yielding. Such improvement can result in reduction of maintenance cost and downtime.

As a remark for implementation, although the conventional design also showed acceptable potential for seismic and wind forces cases, our proposed approach outperformed them when large mass ratios were used. This, however, might present problems to install and maintain as well as the design of the bridge. If because of these issues, the lower mass ratios are selected for a TMD solution, information of the seismic and wind activity of the area should be obtained to decide which design is more effective. In addition, multiple TMD system or smart dampers with different tuning modes could also be used to address this problem.

As the future studies, a more complex problem including 3-dimensional bridge model with various impact force types, angle and heights and multiple-TMD design will be considered. In addition, other factors regarding the cost efficiency of this approach also need to be studied for real life implementation.

7 References

- American Association of State Highway and Transportation Officials. (2012). *AASHTO LRFD Bridge Design Specifications*. Washington, D.C., American Association of State Highway and Transportation Officials.
- Bachmann, H. (1995). *Vibration problems in structures*. Basel, Switz.: Birkäuser Verlag.
- Ctbuh.org, (2015). *Council on Tall Buildings and Urban Habitat*. [online] Available at: <http://www.ctbuh.org/> [Accessed 7 Apr. 2015].
- Cowan, David. 'Development Of Time-History And Response Spectrum Analysis Procedures For Determining Bridge Response To Barge Impact Loading'. Doctor of Philosophy. University of Florida, 2007. Print.
- Dallard, P., Fitzpatrick, A., Flint, A., Le Bourva, S., Low, A., Smith, R. and Willford, M. (2001). The London Millennium Footbridge. *The Structural Engineer*, pp.17-33.
- Den Hartog, J. (1956). *Mechanical vibrations*. New York: McGraw-Hill.
- Farghaly, A. and Salem Ahmed, M. (2012). Optimum Design of TMD System for Tall Buildings. *ISRN Civil Engineering*, 2012, pp.1-13.
- Gerb.com, (2015). *GERB - Projects*. [online] Available at: http://www.gerb.com/en/arbeitsgebiete/projektbeispiele/show_projektbeispiel.php?rubrik=tilger&projekt=millen_b_ridge [Accessed 22 Jan. 2015].
- Gutierrez Soto, M. and Adeli, H. (2013). Tuned Mass Dampers. *Archives of Computational Methods in Engineering*, 20(4), pp.419-431.

- Hoang, N., Fujino, Y. and Warnitchai, P. (2008). Optimal tuned mass damper for seismic applications and practical design formulas. *Engineering Structures*, 30(3), pp.707-715.
- Leung, A. and Zhang, H. (2009). Particle swarm optimization of tuned mass dampers. *Engineering Structures*, 31(3), pp.715-728.
- Meier-Dornberg, K.E., 1983, *Ship Collisions, Safety Zones and Loading Assumptions for Structures in Inland Waterways*. Report No. 496, (Germany: Association of Engineers)
- Meirovitch, L. (1975). *Elements of vibration analysis*. New York: McGraw-Hill.
- Mississippiriverresource.com, (2015). *Mississippi River Facts*. [online] Available at: <http://www.mississippiriverresource.com/River/RiverFacts.php> [Accessed 22 Jan. 2015].
- Nps.gov, (2015). *Mississippi River Facts - Mississippi National River & Recreation Area (U.S. National Park Service)*. [online] Available at: <http://www.nps.gov/miss/riverfacts.htm> [Accessed 30 Apr. 2015].
- Pakrashi, V., O'Connor, A. and Basu, B. (2010). Effect of tuned mass damper on the interaction of a quarter car model with a damaged bridge. *Structure and Infrastructure Engineering*, 6(4), pp.409-421.
- Sadek, F., Mohraz, B., Taylor, A. and Chung, R. (1997). A method of estimating the parameters of tuned mass dampers for seismic applications. *Earthquake Engineering and Structural Dynamics*, 26(6), pp.617-635.
- Sladek, J. and Klingner, R. (1983). Effect of Tuned-Mass Dampers on Seismic Response. *ASCE Journal of Structural Engineering*, 109(8), pp.2004-2009.
- Spencer BF Jr, Christenson RE and Dyke SJ (1998) Next Generation benchmark control problem for seismically excited buildings. In *Proceedings of the Second World Conference on Structural Control*, Kyoto, Japan, June 29-July 2, pp.1351-1360.
- Svensson, H. (2009). Protection of bridge piers against ship collision. *Steel Construction*, 2(1), pp.21-32.
- Taipei-101.com.tw, (2015). *101 Taipei Financial Center Corp.*. [online] Available at: <http://www.taipei-101.com.tw/en/observatory-damper.aspx#SCROLL2> [Accessed 22 Jan. 2015].
- Warburton, G. (1982). Optimum absorber parameters for various combinations of response and excitation parameters. *Earthquake Engineering and Structural Dynamics*, 10(3), pp.381-401.
- Wardhana, K. and Hadipriono, F. (2003). Analysis of Recent Bridge Failures in the United States. *Journal of Performance of Constructed Facilities*, 17(3), pp.144-150.

Yuan, P. (2005). *Modelling, Simulation and Analysis of Multi-Barge Flotillas Impacting Bridge Piers*. PhD.
University of Kentucky.